SANDIA REPORT

SAND2005-2521
Unlimited Release
Printed April 2005

An Aluminum Resist Substrate for Microfabrication by LIGA

S. K. Griffiths, M. W. Losey, J. T. Hachman, D. M. Skala, L. L. Hunter, N. Y. C. Yang, D. R. Boehme, J. S. Korellis, G. Aigeldinger, W. Y. Lu, J. J. Kelly, M. A. Hekmaty, D. E. McLean, P. C. Y. Yang, C. A. Hauck, T. A. Friedmann

Prepared by
Sandia National Laboratories
Albuquerque, New Mexico 87185 and Livermore, California 94550

Sandia is a multiprogram laboratory operated by Sandia Corporation, a Lockheed Martin Company, for the United States Department of Energy's National Nuclear Security Administration under Contract DE-AC04-94AL85000.

Sandia National Laboratories

Issued by Sandia National Laboratories, operated for the United States Department of Energy by Sandia Corporation.

Available to DOE and DOE contractors from
U.S. Department of Energy
Office of Scientific and Technical Information
P.O. Box 62
Oak Ridge, TN 37831

Telephone: (865)576-8401
Facsimile: (865)576-5728
E-Mail: reports@adonis.osti.gov
Online ordering: http://www.doe.gov/bridge

Available to the public from
U.S. Department of Commerce
National Technical Information Service
5285 Port Royal Rd
Springfield, VA 22161

Telephone: (800)553-6847
Facsimile: (703)605-6900
E-Mail: orders@ntis.fedworld.gov
Online order: http://www.ntis.gov/help/ordermethods.asp?loc=7-4-0#online

SAND2005-2521
Unlimited Release
Printed April 2005

An Aluminum Resist Substrate for Microfabrication by LIGA

S. K. Griffiths, M. W. Losey, J. T. Hachman, D. M. Skala, L. L. Hunter, N. Y. C. Yang, D. R. Boehme, J. S. Korellis, G. Aigeldinger, W. Y. Lu, J. J. Kelly, M. A. Hekmaty, D. E. McLean, P. C. Y. Yang, C. A. Hauck[+], T. A. Friedmann[++]

Sandia National Laboratories
Livermore, California 94551-0969

[++]Sandia National Laboratories
Albuquerque, New Mexico 87123

[+]Lawrence Berkeley National Laboratory
Berkeley, California 94720

Abstract

Resist substrates used in the LIGA process must provide high initial bond strength between the substrate and resist, little degradation of the bond strength during x-ray exposure, acceptable undercut rates during development, and a surface enabling good electrodeposition of metals. Additionally, they should produce little fluorescence radiation and give small secondary doses in bright regions of the resist at the substrate interface. To develop a new substrate satisfying all these requirements, we have investigated secondary resist doses due to electrons and fluorescence, resist adhesion before exposure, loss of fine features during extended development, and the nucleation and adhesion of electrodeposits for various substrate materials. The result of these studies is a new anodized aluminum substrate and accompanying methods for resist bonding and electrodeposition. We demonstrate successful use of this substrate through all process steps and establish its capabilities via the fabrication of isolated resist features down to 6 μm, feature aspect ratios up to 280 and electroformed nickel structures at heights of 190 to 1400 μm. The minimum mask absorber thickness required for this new substrate ranges from 7 to 15 μm depending on the resist thickness.

Introduction

Microfabrication by the LIGA* process employs deep x-ray lithography and electrodeposition to produce small metal or plastic parts having lateral dimensions up to several centimeters and feature sizes down to one micrometer or less [1-3]. To fabricate such parts, a thick x-ray resist is bonded or cast onto a conductive substrate and exposed to synchrotron radiation through a

* From the German *Lithographie, Galvonoformung und Abformung*

patterned mask. This resist, usually polymethyl methacrylate (PMMA), is subsequently developed to form a patterned non-conducting mold attached to the substrate. The mold is then filled by electrodeposition to form either individual metal parts or a metal die for replicating plastic parts by embossing or injection molding. To make individual parts, the top surface of the mold is planarized after electrodeposition, the resist is chemically removed, and the finished parts are released from the substrate. This abbreviated process is illustrated in Figure 1. To create a replication die, the mold is typically overfilled, the top-surface of the over-plate is planarized, and the substrate and resist are then removed.

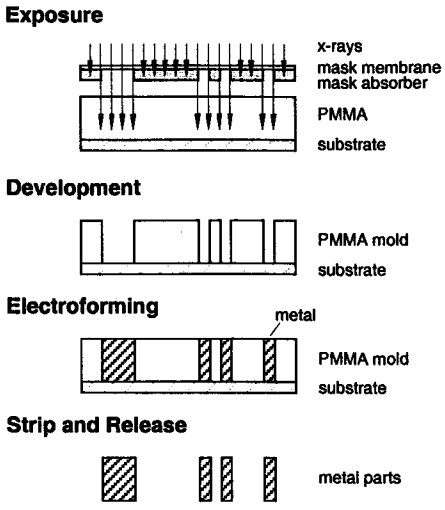

Figure 1. Illustration of the LIGA process as applied to the fabrication of metal parts. When making individual parts, the top surface of the mold is planarized (as shown) following electrodeposition.

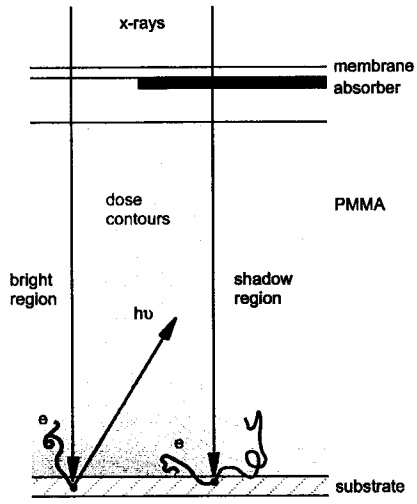

Figure 2. Schematic of mask, resist and substrate. X-rays absorbed in the substrate produce electrons and fluorescence yielding extraneous shadow-region doses and high doses at the substrate interface.

The conductive substrate carrying the x-ray resist serves several critical functions in the LIGA process. It must first hold isolated resist features in their correct relative positions following development and throughout the plating process. PMMA thermal expansion and the absorption of water during these process steps produce large stresses at the substrate interface, so a strong bond between the resist and substrate surface is required to avoid resist delamination and the loss of features. The substrate must also serve as an electrical conductor capable of providing a uniform potential at the deposition surface of all mold cavities. Non-uniform electric potentials contribute to non-uniform electrodeposition, and such non-uniformity creates problems in filling some mold cavities without overfilling others. Finally, the substrate must provide ready nucleation of electrodeposits and good adhesion of the deposited metal. Poor nucleation promotes bubble formation during electrodeposition, leading to voids in metal parts, while poor adhesion results in the loss or destruction of metal structures during planarization.

Substrates additionally affect the LIGA process during x-ray exposure of the resist. As depicted in Figure 2, primary x-rays from the synchrotron source can pass through the mask membrane and the mask absorber when the photon energy is high. Such high-energy photons likely pass through the resist as well, but may be absorbed in the substrate below due to the relatively high

x-ray cross-sections of most substrate materials. This absorption yields high-energy photoelectrons and Auger electrons that can leave the substrate, enter the resist, and produce large secondary doses (>100 J/cm^3) in a very thin layer of the resist adjacent to the substrate surface [4-6]. The thickness of this layer is typically a few micrometers. Such shadow-region interface doses may lead to loss of adhesion through dissolution of the interface during development or through mechanical failure due to radiation-induced degradation of bond strength [5,7]. Increasing the mask absorber thickness reduces shadow-region interface doses [8], but increased absorber thickness degrades feature tolerances and limits producible feature sizes due to inherent limitations of the mask-making process. This is especially a concern for x-ray masks fabricated by means of ultraviolet (UV) lithography. Masks produced using UV lithography exhibit feature tolerances and a minimum producible feature size that are limited by diffraction, and these grow roughly in proportion to the square-root of the absorber thickness. For a UV source having a characteristic wavelength λ = 365 nm, the diffraction-limited size based on resolution is roughly $d \approx 1.1\sqrt{\lambda\delta} \approx 4$ μm for an absorber thickness of $\delta = 40$ μm; it is only 2 μm for a 10 μm thickness. A thin absorber additionally reduces plating-induced stresses in the mask membrane, improving mask accuracy through reduced mask deformation. Alternatively, reduced stresses permit the use of a thinner, more transparent mask membrane, and this generally improves the tolerances of developed resist features by transmission of a softer x-ray spectrum.

X-rays absorbed in bright regions of the substrate also produce secondary emissions capable of impacting the process. Here, photons passing through the mask membrane and resist may be absorbed in the substrate, and this again produces high-energy electrons leading to a high resist dose at the substrate interface. Unlike their shadow-region counterparts, however, bright-region interface doses can be extremely large (~100 kJ/cm^3) since the mask absorber removes none of the primary spectrum. Such extreme doses produce a thin layer of insoluble resist adjacent to the substrate, and this layer must be removed by a post-development etch. Post-development etching roughens the sidewalls of resist features and is thus unacceptable for most optical applications of the process. X-rays absorbed in bright regions of the substrate can also generate fluorescence radiation. In contrast to electrons, fluorescence photons are absorbed over large distances ranging up to several millimeters. Since fluorescence is emitted isotropically, some of this radiation is absorbed by the resist in regions shaded by the absorber. During subsequent development, this extraneous dose can lead to substantial dissolution of feature sidewalls, resulting in discrepancies between the mask pattern and the developed mold geometry [7,9,10]. Fluorescence is also produced in shadowed regions of the substrate, but this is usually unimportant due to the much lower primary doses.

In the present paper, these various requirements for a good resist substrate are examined using both theoretical and experimental methods. We report the computed influence of substrate material on secondary doses and required mask absorber thickness, measurements of initial resist bond strength and post-exposure feature loss, and experimental studies of electrodeposition directed at good nucleation and adhesion of metal structures. We also describe the successful development of an anodized aluminum substrate satisfying all important requirements and demonstrate use of this substrate in producing small resist features of high aspect ratio and electroformed structures containing fine isolated negative details.

Past Research

Early accounts of the LIGA process by Becker *et al.* describe substrates consisting of thick steel or copper plates coated with gold, titanium or nickel [1]. To improve adhesion, the surfaces of these substrates were roughened by microgrit blasting or wet oxidation. Steel and copper substrates were soon replaced with oxidized titanium disks or wafers metallized with a titanium film and oxidized to produce significant surface roughness [3,11]. Oxidized titanium provided good PMMA adhesion and a good surface for electrodeposition. Applied to glass or silicon wafers, titanium films further provided a sacrificial layer for the release or partial release of parts at completion of the process. Variants of this titanium oxide substrate have been used widely and successfully ever since. Nevertheless, substrate technology has remained a topic of significant research.

Guckel *et al.* [12,13] likewise proposed a substrate formed by metallizing a glass or silicon wafer. Their silicon wafer was first roughened by surface oxidation and then metallized with titanium and nickel to produce a conductive surface. The nickel surface served as a plating base, while the titanium film provided a sacrificial layer for removal of the metal parts. They further suggested bonding PMMA sheets to the substrate using a thin spin-cast layer of PMMA applied to the substrate surface [14-16]. The PMMA sheet was then solvent-bonded to this layer using methyl methacrylate monomer. Guckel *et al.* later proposed a substrate consisting of a silicon wafer metallized with titanium, copper and more titanium [17]. Here the outer titanium was removed by etching to expose a copper base before electrodeposition, and the copper film served as a sacrificial layer for part release. This substrate has also been widely used, despite some rather severe limitations. The large x-ray cross-section of copper limits this substrate to use with soft x-ray spectra since harder spectra require an excessive absorber thickness to avoid loss of adhesion. In addition, this substrate usually requires a preliminary de-scum etch after development to remove insoluble PMMA adjacent to the substrate, owing again to the large cross-section of copper.

Recognizing the importance of secondary doses, several investigators have since studied the effects of the x-ray spectrum and substrate materials on PMMA adhesion. Using theoretical and experimental means, Pantenburg *et al.* demonstrated that doses in the resist adjacent to the substrate and the associated loss of features were strongly dependent on the x-ray critical energy when the substrate and absorber thickness are fixed [4] and that adhesion can be improved significantly by increasing absorber thickness [8]. Schmidt *et al.* similarly demonstrated that adhesion depends strongly on the substrate material for fixed absorber thickness and fixed x-ray energy [5]. In this study, they investigated copper, titanium, vitreous carbon and gold substrates and showed that the post-exposure PMMA bond strength decreased dramatically with increasing atomic number of the substrate material. Under their conditions, the measured bond strength for the titanium substrate was about 65% of that for carbon; the strength for copper was about half that for titanium.

Kadereit *et al.* examined the effect of adhesion promoters on post-exposure bond strength for substrates consisting of silicon or ceramic wafers metallized with aluminum or titanium oxide [18]. They showed that the titanium oxide film on either wafer provided high bond strength with sufficient concentration of the promoter, while the aluminum film gave very low

bond strengths regardless of the promoter concentration. Malek and Das also examined adhesion promoters and other factors influencing the initial bond strength prior to exposure for titanium, titanium oxide, copper, copper oxide and gold films applied to silicon wafers, and they again showed the importance surface roughness in obtaining high bond strength [19]. This was further demonstrated in the work of Kanigicheri *et al.* using copper disks treated to produce a surface coating of black copper oxide [20].

Using a different approach, De Carlo *et al.* solved the problem of high interface doses by incorporating a polymer buffer layer between the metallic surface and the resist [21-23]. The thin buffer layer, insoluble in developer and not degraded by radiation, absorbs electrons emitted by the metal before they reach the resist. This ensures that the PMMA bond strength is not degraded during exposure, but the buffer layer must be removed by etching before electrodeposition.

While PMMA adhesion has been reasonably well studied, only a few studies have addressed the equally important issue of adhesion between the substrate and electrodeposited metal. Kunz *et al.* examined the adhesion of nickel to ceramic wafers metallized with layers of chrome and gold [24]. They demonstrated that adsorbed water on the ceramic surface and the temperatures used for depositing the metal films played important roles in metal adhesion. El-Kholi *et al.* investigated both PMMA and metal adhesion for silicon wafers coated with carbon or metallized with oxidized titanium [25]. They showed superior adhesion of the PMMA for the carbon coating following x-ray exposure, though metal adhesion to the carbon for electrodeposited nickel, copper and gold was very poor. Metal adhesion was improved by patterning the carbon with small platinum dots prior to bonding the PMMA resist. This patterned platinum slightly degraded PMMA adhesion. Finally, Makarova *et al.* successfully demonstrated use of a monolithic graphite substrate in producing tall copper structures [26]. They attributed the good performance of this substrate to the low x-ray cross-section of carbon and the micro-porous roughness of the graphitic carbon surface.

Secondary Doses

Photoelectrons and Auger electrons produced in the substrate are the dominant source of secondary doses leading to post-exposure loss of adhesion. To maintain these doses at acceptable levels, the absorber thickness must exceed some minimum value that depends on the resist thickness, characteristics of the substrate material, and the energy spectrum of the incident x-ray beam. Again, a small absorber thickness is preferred for high accuracy or for producing very small features.

X-ray cross-sections are the main characteristic of substrate materials affecting secondary doses and the minimum absorber thickness. This is because the dose in the resist adjacent to the substrate is roughly proportional to the dose absorbed in the substrate whenever the cross-section of the substrate is much larger than that of PMMA. Since this is usually the case, substrates exhibiting reduced x-ray cross-sections generally yield lower interface doses and so permit a reduced absorber thickness. Cross-sections for several materials of interest are plotted in Figure 3. Here we see that the cross-sections of titanium and titanium oxide at high photon energies (>10 keV) are factors of about 4 and 6 smaller than those of copper, nickel and zinc.

Cross-sections of aluminum and aluminum oxide are about a factor of 7 less than those of titanium, and those of carbon and beryllium are at least an order of magnitude below those of aluminum.

Because x-ray cross-sections for all materials depend on the photon energy, the source x-ray spectrum also affects adhesion and minimum absorber thickness [27], and this effect is dominated by the highest photon energies. Thus, if the spectrum is tailored using a beam-line mirror to remove energies above 8 keV, then copper, nickel, zinc, titanium and titanium oxide substrates should yield similar values of the minimum absorber thickness since the cross-sections of these materials are all similar at energies just below 8 keV. Likewise, if the spectrum is tailored to remove energies above 4 keV, then titanium and titanium oxide substrates should give values of the minimum absorber thickness comparable to those for aluminum and aluminum oxide. This is also apparent in Figure 3.

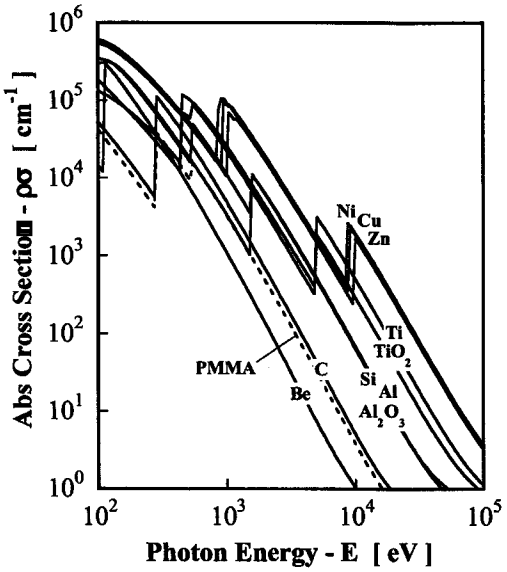

Figure 3. Absorption cross-sections for various materials of interest for use as substrates or as substrate metallization layers. Reduced cross-sections generally permit reduced mask absorber thickness.

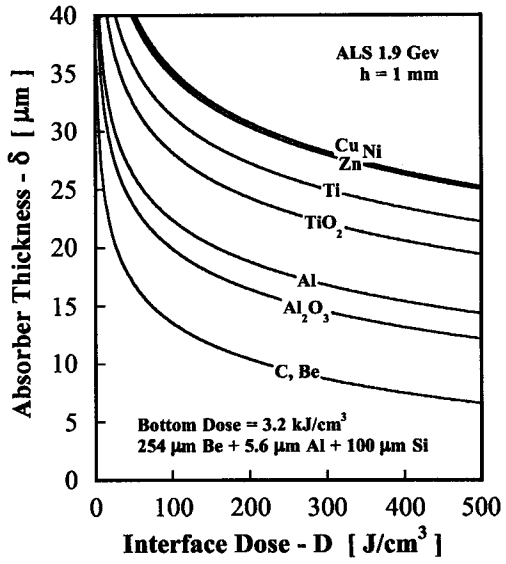

Figure 4. Computed minimum absorber thickness as a function of allowable interface dose for various substrate materials at a resist thickness of 1 mm and exposure at ALS operating at 1.9 GeV.

Sample calculations showing the minimum gold absorber thickness as a function of the acceptable interface dose are presented in Figure 4. These results were computed using Sandia's LEX-D code [10,28,29] for a PMMA resist thickness of 1 mm and exposure at the Advanced Light Source (ALS) operating at 1.9 GeV (E_c = 2.99 keV). The x-ray beam is filtered by 254 μm of beryllium, 5.6 μm of aluminum, 0.13 m of air and a 100 μm silicon mask membrane. The work by Schmidt *et al.* suggests that interface doses should not exceed about 100 J/cm^3 based on degradation of PMMA strength [8]. Using this criterion, Figure 4 indicates that the minimum absorber thicknesses for nickel, copper and zinc substrates slightly exceed 35 μm. Minimum thicknesses for titanium and titanium oxide are about 31 and 28 μm, respectively, and those for aluminum and aluminum oxide are about 22 and 20 μm. For carbon and beryllium, the interface dose is less than the resist primary dose, and the primary dose is not influenced by the substrate.

The minimum thickness for both these materials is thus about 14 μm, based on a primary dose of 100 J/cm^3 near the bottom of the resist.

Degradation of bond strength may be a secondary concern if the initial bond strength is very high. In this case, much larger doses at the substrate interface may be tolerable since post-exposure bond strength need only exceed the maximum stresses induced during development and electrodeposition. However, large doses yield large resist dissolution rates, and the undercut of features by lateral dissolution also leads to feature loss if the interface dose is too large. The undercut rate thus provides a second, more lenient criterion for the acceptable interface dose and associated minimum absorber thickness. Computed undercut rates are shown in Figure 5 as a function of absorber thickness for cross-linked PMMA and various substrate materials. These dissolution rates [29,30] are based on the interface doses given previously in Figure 4 for development at 21 °C.

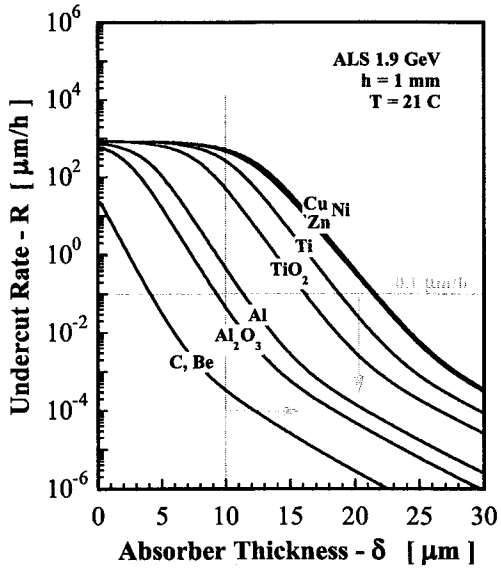

Figure 5. Computed undercut rates for lateral dissolution at the substrate interface. Undercut rates below 0.1 μm/h are required for challenging applications of LIGA.

Figure 5 demonstrates that undercut rates are extremely sensitive to absorber thickness for any given substrate material. Indeed, a variation in absorber thickness of just over 2 μm alters the undercut rate by an order of magnitude on the steepest portions of these curves. Undercut rates are likewise very sensitive to the substrate material for any fixed absorber thickness, and these rates span the range from negligibly small to wholly unacceptable. Within this range, the horizontal line in Figure 5 indicates a marginally acceptable value of 0.1 μm/h. This would allow, for example, over-development of isolated 5 μm posts by up to 25 hours, as required for a 1 mm resist also pattered with negative features of this size. At this acceptable rate, the minimum absorber thicknesses for copper, nickel and zinc substrates are all about 22 μm. Equivalent minimum thicknesses for titanium, titanium oxide, aluminum and aluminum oxide are 19, 16, 11 and 9 μm, respectively, while those for carbon and beryllium are only about 4 μm. Note that these thicknesses are significantly smaller than those in Figure 4 because a dissolution rate of 0.1 μm/h at 21 °C corresponds to an interface dose of 1.2 kJ/cm^3 for cross-linked PMMA (about 900 J/cm^3 for linear PMMA). While such a dose seems extremely large in view of the work by Schmidt *et al.* [8], it is nevertheless similar to the acceptable doses determined by Pantenburg *et al.* for the exposure of thin 20 μm resists used in making masks [4]. Their values

ranged from 2 to 3 kJ/cm^3, yielding undercut rates between 1.3 and 8.7 μm/h. These higher rates may have been acceptable for their application because development times for a 20 μm resist are very small, about 10 minutes, and over-development times should be likewise very small since development rates are insensitive to feature size for this small resist thickness.

Even if the undercut rate is sufficiently low, absorber thicknesses less than about 10 μm are not generally acceptable because they provide inadequate dose contrast and so lead to significant dimensional errors [28]. An absorber thickness of 10 μm yields a top-surface shadow-region dose about 0.3 kJ/cm^3 for the conditions of Figure 5, and this is just at the threshold for significant sidewall dissolution [28,29]. The vertical line in Figure 5 denotes this minimum absorber thickness based on dimensional errors. Thus, if the absorber thickness is constrained by both the undercut rate and dimensional accuracy, there is little or no difference between the expected benefits of carbon, beryllium, aluminum oxide and aluminum substrates. They all require an absorber thickness of about 10 μm. In contrast, the remaining substrate materials, including oxidized titanium, require a larger absorber thickness that is determined by the undercut rate alone.

The interface doses shown in Figure 4 and used in computing the undercut rates of Figure 5 are based on a monolithic substrate or metallization layer that is thick compared to the effective range of the electrons produced in the metal. In this limit, interface doses for given exposure conditions are independent of the substrate thickness, and this limiting behavior for most metals arises at a thickness exceeding 200 nm for the exposure conditions of Figures 4 and 5. As such, there should be no difference in the expected performance of a monolithic metal substrate and a metallized wafer if the thickness of the metallization layer is more than about 200 nm. Interface doses can be reduced, however, if the metallization layer is extremely thin and if the cross-section of the underlying material is significantly less than that of the metal layer. This opens the possibility of a multi-layer substrate consisting of a conductor such as an aluminum disk or aluminized silicon wafer that is coated with a very thin layer of copper, zinc or nickel to provide a more suitable surface for electrodeposition. The thickness of this seed layer in such a scheme needs to be less than about 10 nm to avoid significant contributions to the interface dose.

In addition to their influence on resist adhesion, substrates affect sidewall tolerances through the emission of fluorescence from bright regions [10]. Fluorescence yields for copper, zinc and nickel are 0.44, 0.47 and 0.40; those for titanium and aluminum are 0.24 and 0.04. Fluorescence yields for carbon and beryllium are negligible. Based on these values, the cross-sections of Figure 3, and the exposure conditions of Figure 4, computed maximum shadow-region fluorescence doses at the substrate interface in a PMMA resist are 520, 440 and 560 J/cm^3 for copper, zinc and nickel. The doses for titanium and titanium oxide are 490 and 120 J/cm^3, while those for aluminum and aluminum oxide are 70 and 8 J/cm^3, respectively. These values are based on a thick monolithic substrate. Maximum shadow-region fluorescence doses for a 3 μm substrate metallization layer are roughly 40% smaller. Sidewall terminal doses at the end of development for a 1 mm resist developed at 21 C are about 300 J/cm^3 for linear PMMA [29], so sidewall dimensional errors due to fluorescence from aluminum, aluminum oxide and titanium oxide should be very small. Sidewall errors for copper, nickel, zinc or titanium substrates may be large [10].

Finally, electrons emitted from bright regions of the substrate may produce doses in the resist sufficiently large that a thin resist layer at the substrate interface becomes insoluble in the developer [31]. Bright-region doses in a PMMA resist at the substrate interface for copper, zinc and nickel substrates are roughly 100 kJ/cm^3 (note kiloJoules) for the exposure conditions of Figure 4. These doses are 88, 52, 20 and 12 kJ/cm^3 for titanium, titanium oxide, aluminum and aluminum oxide, respectively. Copper and nickel are known to produce insoluble resist layers, so zinc will too and titanium may also under some conditions. Titanium oxide does not produce an insoluble layer for these conditions, so neither will aluminum, aluminum oxide and carbon.

Feature Loss and Resist Adhesion

To assess the effects of secondary doses by experimental means, we conducted post-exposure PMMA loss-of-features studies using several candidate substrates. Exposures for these studies were performed at ALS operating at 1.9 GeV using a test mask formed on a 100 μm silicon wafer. The mask absorber thickness was either 18 or 34 μm, and the resist thickness was typically 750 μm. Following exposure, the resist was developed for an extended period, and the loss of PMMA features was noted as a function of time. The substrates tested in this way included vitreous carbon and aluminum disks, aluminum disks coated with oxidized titanium, silicon wafers metallized with aluminum or titanium oxide, silicon wafers metallized with both aluminum and titanium, and glass wafers metallized with aluminum. Silicon wafers metallized with titanium, copper and titanium (Ti-Cu-Ti) were also investigated.

In these studies, annealed PMMA sheet was bonded to the substrates using either solvent [32] or a PMMA-based glue [20,33] developed at Forschungszentrum Karlsruhe (FZK). For solvent bonding, a 2 μm layer of PMMA (950 kg/mol) was first applied to the substrate by spin casting. The PMMA sheet was then bonded to the cured spin layer using methyl methacrylate (MMA) monomer. For gluing, the adhesive consisted of 10 g of 15% by weight PMMA (950 kg/mol) in MMA, 0.1 g N,N-dimethyl aniline, 0.1 g 3-(trimethoxylsilyl)propyl methacrylate (MEMO), and 0.1 g benzoyl peroxide. This was degassed under a vacuum of 22 mmHg for a few minutes before application, and the bond interface was loaded to 450 kPa (65 psi) with a press and glass platens for a minimum of four hours.

Sample results are shown in Figures 6 and 7. For all these results, the PMMA was solvent bonded to the substrate, the absorber thickness was 18 μm, and the x-ray beam was filtered as specified for Figure 4. The primary dose at the bottom of the PMMA was 4.0 kJ/cm^3 (based on E_c = 3.16 keV) for Figure 6 and the Ti-Cu-Ti and Al-Ti substrates in Figure 7. Bottom doses for all other substrates in Figure 7 were 3.2 kJ/cm^3.

Figure 6 shows test features remaining on a substrate wafer metallized with aluminum (bottom) and one metallized with Ti-Cu-Ti (top) following 24 hours of development. For these features, this corresponds to over-development by roughly 17 hours, as required for full development of small negative features also patterned in the resist. We see that the aluminum substrate in Figure 6 exhibits no loss of features down to the smallest 10 μm size, while the Ti-Cu-Ti displays feature loss for sizes of 150 μm and below at the same development time. After 122 hours of

development, the aluminized substrate showed feature loss only at 50 μm and below. At this time, no features remained on the Ti-Cu-Ti.

Figure 7 illustrates the average size of features lost as a function of development time for various feature geometries and a range of substrate materials. These curves confirm the benefit of low x-ray cross-sections in reducing feature loss after exposure: the best results were obtained using the carbon substrate; aluminum substrates and aluminized wafers provided minimal loss of features even for extended over-development; and wafers metallized with Ti-Cu-Ti displayed significant loss of features beginning just at the end of development and a high rate of loss of larger sizes with increasing development time. These results also demonstrate that feature loss for the multi-layer Al-Ti metallization depends on the thickness of the titanium layer. Reducing this thickness from 80 to 10 nm significantly reduced feature loss. Similar loss-of-features tests for aluminum substrates and resists bonded using PMMA glue displayed no loss of features for feature sizes of 7 μm and larger over comparable development times.

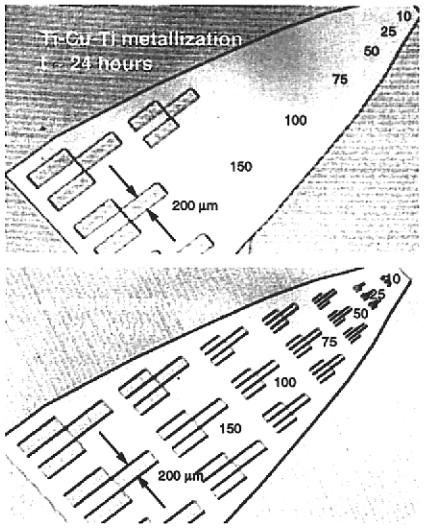

Figure 6. Optical images of PMMA features during development. Substrates metallized with aluminum (bottom) and Ti-Cu-Ti (top) show widely different feature loss for the same exposure conditions.

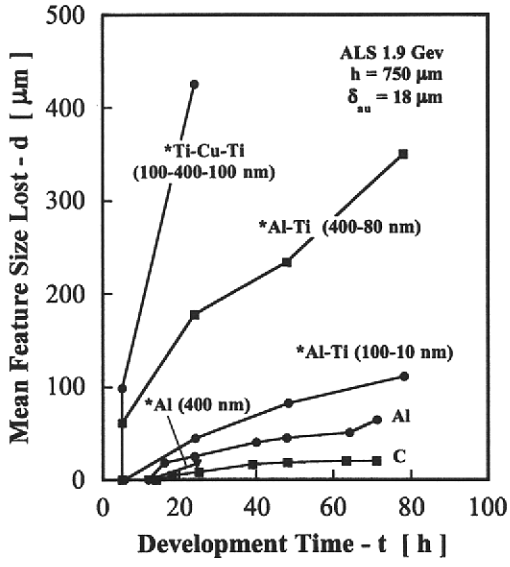

Figure 7. Average feature size lost as a function of time for several substrates. Asterisk denotes metallization on a silicon wafer; no asterisk denotes thick monolithic substrates.

These adhesion studies also revealed that solvent bonding tended to produce anomalous results in that small PMMA features remained attached to the substrate, while larger features elsewhere on the substrate were lost. This unexpected behavior appears to originate in stochastic spatial variations of the initial bond strength over the resist area. That is, large features are lost from varying portions of the test pattern from one test to the next. We attribute such behavior to waviness of the PMMA. Film thickness measurements of the PMMA spin-cast layer indicate uniformity of thickness to within 40 nm. In contrast, the PMMA sheet exhibits waviness on the order of tens of micrometers, and this is not removed by annealing. Local variations in the PMMA surface can therefore lead to local bond regions that are rich or lean in the methyl methacrylate solvent, producing a non-uniform bond on length scales sufficient to impact feature

loss. These anomalous results were rarely seen when the resist was bonded using PMMA-based glue.

While loss of features tends to be most problematic for small features and thick resists, delamination usually occurs in areas where the lateral expanse of resist is large compared to the resist thickness and when the resist thickness is small. This is because delamination arises from stresses induced by PMMA thermal expansion and the absorption of water from the developer or electrolyte bath. For a given homogeneous strain, shear stresses at the interface between the resist and substrate reach a maximum value that is independent of thickness when the lateral feature size is more than three times the resist thickness. In this limit, the time to reach maximum interface stress increases roughly with the square of the resist thickness [34] so thin resists having features of low aspect ratio reach maximum stress earlier in the period of development or electrodeposition. As such, they are more prone to delamination and thus require a higher bond strength.

To investigate characteristics affecting initial bond strength, we conducted a series of pre-exposure pull tests using various substrates and various surface preparations. In these tests, six PMMA tabs were bonded to candidate substrates and pulled in a lap-shear manner using a test frame and a calibrated load cell to measure the pulling force. The effective bond strength was then calculated by dividing the maximum pulling force by the bond area. Tests of this sort were performed on aluminum discs and silicon wafers coated with aluminum, etched aluminum, anodized aluminum, titanium, oxidized titanium* and Ti-Cu-Ti. The surface roughness of these substrates was also characterized.

Measured bond strengths and the corresponding surface roughnesses are shown in Figure 8 for seven of these substrates. The strengths vary from 2 MPa to at least 56 MPa, depending on the substrate surface. Surface roughnesses range from 3 to almost 900 nm. These strengths are consistent with the values measured by Kadereit *et al.* [18], but are significantly lower than those reported by Schmidt *et al.* [5]. However, the highest bond strengths could not be measured here because the PMMA tab failed instead of the bond line. In such cases, the calculated bond stress at tab failure represents a minimum bond strength, as indicated by the arrows in Figure 8.

Figure 8 suggests that bond strength correlates well with surface roughness. The obvious exception to this is the rough aluminum (rightmost bars) which exhibits high roughness but only moderate strength. For this aluminum, however, the lateral scale of the roughness is very much larger than that of titanium oxide and anodized aluminum. This is illustrated in Figure 9 depicting substrate surface characterization by white-light interferometry. Here light areas denote elevated regions; dark areas represent regions that are low. High frequency roughness on the sub-micron scale is evident in the titanium oxide and anodized aluminum, indicating a large surface area, but this is absent in the rough aluminum. The scale of the roughness thus also plays an important role in resist adhesion, at least when the scale deviates significantly from that of oxides.

---

* Oxidized in 900 ml deionized water, 19 ml 30% hydrogen peroxide and 19 g sodium hydroxide at 60 °C. Dried at 100 °C.

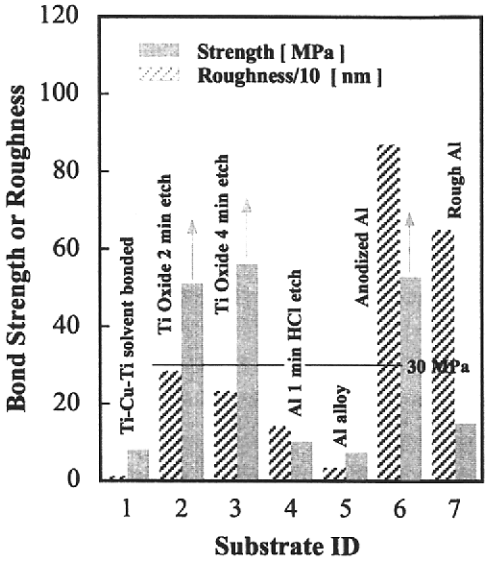

Figure 8. Bond strength and RMS surface roughness for various substrates and surface preparations. Strength correlates well with roughness except in the case of rough aluminum. Roughness is scaled by 10.

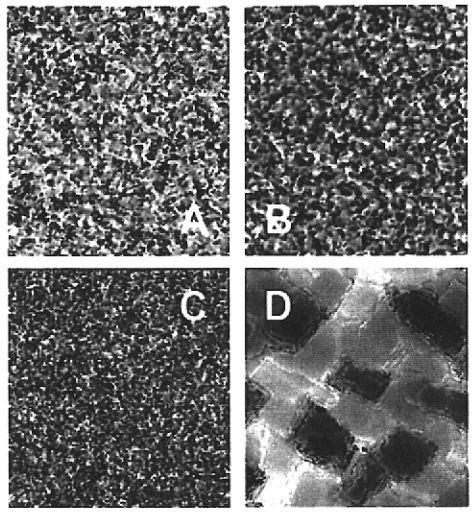

Figure 9. White-light interferometric images of titanium etched for 2 minutes (A) and 4 minutes (B), anodized aluminum (C) and rough sputtered aluminum (D). Width of each image is 35 μm.

The horizontal line in Figure 8 at 30 MPa represents our current estimate of the minimum bond strength required to avoid delamination. This value, independent of the resist thickness, is the maximum stress computed for several geometries based on a PMMA Young's modulus of 3 GPa and a total strain of 0.4% for combined thermal expansion and water absorption [35,36]. Thus, of the substrates shown, only the oxidized titanium and anodized aluminum provide sufficient bond strength even prior to x-ray exposure. Since exposure always degrades bond strength, some margin is additionally required. This margin is at least a factor of two for titanium oxide and anodized aluminum, but probably not much more since the tensile strength of PMMA is at most 80 MPa.

Electrodeposition

Based on the theoretical results presented above and conclusions drawn from these adhesion studies, our effort examining electrodeposition concentrated on carbon and aluminum substrates. As a screening test, substrate samples were prepared, a thin layer of copper was deposited on the surface, and the deposited metal was evaluated for uniformity of nucleation and adhesion. Adhesion was measured using a calibrated tape peel test. Lapped vitreous carbon disks and carbon-coated silicon wafers were among the first substrates tested in this way. These gave poor nucleation, poor metal adhesion, or both. Graphitic carbons were not considered in depth here based on their poor mechanical properties and the concern that metal structures would become detached or damaged during planarization. This apprehension was affirmed by a single test.

In light of these problems with carbon, and similar problems encountered elsewhere [25], we focused exclusively on aluminum and pursued several novel approaches to plating on aluminum

in the context of LIGA. One such approach was to coat the aluminum with an extremely thin layer of zinc prior to bonding the resist. The intent of this was to provide a suitable seed layer for electrodeposition, while limiting secondary doses due to the zinc by keeping the thickness of the layer less than about 10 nm. These experiments were not very successful in that nucleation was not sufficiently improved, and thicker seed layers would not be acceptable.

Electroplating on aluminum is a common but somewhat difficult process that is usually approached either through anodization or a zincate process [37,38]. These preparatory processes must be done immediately before electrodeposition, however, and this is problematic for LIGA. Here the anodization or zincate step must be performed through the patterned resist following development, and such through-mold processes are hindered by transport limitations for thick resists if feature aspect ratios are large. The zincate process cannot be completed, in any case, before the resist is adhered to the substrate since a thick zinc layer adjacent to the resist is unacceptable during exposure. Nevertheless, such through-mold processing for both anodization and zincate was attempted with limited success. Nucleation was good but somewhat non-uniform, metal adhesion was moderate to poor, and there were problems with bubble formation within mold cavities, especially for anodization.

Performing the preparatory anodization on an aluminum substrate before bonding the resist is thus an extremely attractive alternative to the through-mold process. This approach helps ensure uniform surface preparation and eliminates a critical process step on high-value resists following exposure and development. It further provides excellent small-scale surface roughness for attaining high resist bond strength. The challenge here is that the surface of the aluminum activated by anodization tends to become inert with time, inhibiting nucleation of electrodeposits.

To overcome this problem, we conducted anodization and electrodeposition experiments using a wide variety of aluminum substrates in the forms of both monolithic disks (1100, 2024, 3003, 5052, 6061 and 7076 alloys) and silicon wafers metallized with high-purity aluminum and aluminum alloys. These experiments revealed that traces of copper in the aluminum composition play a critical role in improving subsequent nucleation. Good nucleation on aluminum surfaces anodized before bonding the resist was obtained for any copper concentration above 1% by weight. Copper concentrations up to about 3% have little effect on secondary doses, so preferred concentrations range from 1 to 3%. Aluminum sheet and sputter targets for metallization having compositions in this range are widely available. Some of these alloys also contain a trace concentration of silicon (>1%) that promotes increased surface roughness and so improves metal adhesion. These experiments also demonstrated that adhesion of the electrodeposited metal depends strongly on the conditions of anodization.

The anodization process is performed in a glass vessel using phosphoric acid that is filtered and stirred vigorously. A lead sheet serves as the cathode. For most of the anodization period, the potential is held constant in the range from 10 to 75 V, but the maximum current is also limited. This produces an initial transient as the potential ramps to the set-point value. For a current limit of 25 mA/cm^2, the potential ramps to a set-point of 50 V in 10 to 20 s depending on the alloy content of the aluminum. Total anodization time is varied from 2 to 10 minutes, producing a porous layer of aluminum oxide up to several micrometers thick depending on the temperature

and electric potential. This layer is shown in Figure 10. Phosphoric acid concentrations of at least 3%, temperatures of at least 22 °C, and an electric potential of at least 10 V give acceptable nucleation but rather poor adhesion. A higher acid concentration of 15%, a temperature of 32 °C, and an applied potential of 75 V provides both good nucleation and good adhesion of the deposited metal to the anodized aluminum surface. Following anodization, substrates are immersed in boiling water for 15 minutes, air dried, and then stored in dry nitrogen prior to bonding the resist.

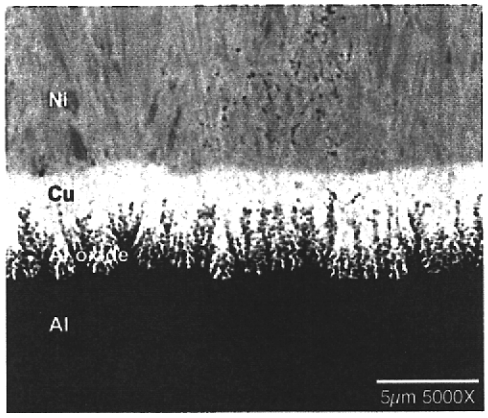

Figure 10. Back-scatter SEM image of a cross-section through an anodized aluminum film with deposited copper and nickel. Aluminum oxide structures provide good metal adhesion.

Prior to through-mold electrodeposition on the anodized substrate, cavities in the patterned resist are filled with degassed, deionized water by immersion under vacuum. To do this, the resist is suspended above a container of water inside a vacuum vessel, and the vessel is evacuated. The resist is then lowered into the water, while still under vacuum, and the pressure is raised to ambient. This ensures complete filling of all mold cavities, without the possibility of trapped bubbles, even for very small cavities of high aspect ratio. The substrate and resist is then transferred to a copper electrolyte bath and allowed to soak without applied current for a period sufficient to ensure full diffusion of electrolyte into the water-filled mold cavities. The approximate minimum soak time is given by $t \approx 0.8 h^2 / D$ where h is the resist thickness and $D \approx 10^{-9}$ m^2/s is a diffusivity characteristic of metal ions in water. This yields about 15 minutes for a resist thickness of 1 mm. A soak time of 30 minutes is thus suitable for most resists.

Following this soak period, a current is applied and gradually increased from 0.1 to 6 mA/cm^2 over about one minute. The current is then held constant at 6 mA/cm^2 for a period sufficient to produce a copper deposit having a thickness of several micrometers. This copper layer, also apparent in Figure 10, serves as a sacrificial layer for part release following planarization. The electrolyte used for this process is copper pyrophosphate (300 g/*l* $K_4P_2O_7$, 84 g/*l* $Cu_2P_2O_7$, 10 g/*l* KNO_3, 8 ml/*l* NH_3OH) maintained at 50 °C and a pH of 8.5. Anodes used here consist of a titanium basket filled with high-phosphorous copper pellets.

After depositing the copper layer, the resist is transferred to de-ionized water and then to de-ionized water that is pH-adjusted using sulfuric or sulfamic acid. The pH of this second solution is matched to the pH of the final bath used in forming the metal structures, *e.g.* pH 3.5 for most nickel electrolytes. This ensures that water or high-pH copper pyrophosphate remaining in mold cavities does not precipitate solids from the low-pH electrolyte when the resist is immersed in the final bath. Again, the duration of this pH-adjusted soak must be sufficient for full

displacement of any residual water or pyrophosphate. A period of 30 minutes is usually adequate. The substrate and resist are then ready for electroforming metal structures using any desired electrolyte bath.

Demonstration of Capabilities

The results of these studies show that an aluminum substrate offers very large advantages in resist adhesion and minimum absorber thickness over monolithic substrates of copper, nickel, zinc or titanium and over wafer-based substrates metallized with titanium or Ti-Cu-Ti. Aluminum may also provide significant advantages over substrates using oxidized titanium or oxidized titanium films. These studies additionally establish that gluing the resist to the substrate provides more consistent adhesion of developed features than does solvent bonding. Finally, they indicate that anodizing an aluminum alloy of the correct composition before bonding the resist provides good resist adhesion, good nucleation of electrodeposits, and good adhesion of metal structures. These favorable attributes of gluing the resist to an anodized aluminum substrate are demonstrated, in part, below.

Using a mask patterned with absorbers of variable thickness, we conducted one test to determine a preliminary value of the required minimum absorber thickness. Four absorber thicknesses were present on this mask (7, 10, 15 and 19 μm); its membrane consisted of a 100 μm silicon wafer. The resist thickness was 750 μm, exposure was performed at ALS operating at 1.9 GeV, the beam was additionally filtered by 254 μm of beryllium, 5.6 μm of aluminum and 0.13 m of air, and the bottom-surface primary dose was 3.2 kJ/cm^3. The exposed resist was developed for a total of 63 hours, but was examined at intermediate times. It was photographed in the wet state at these intermediate times and again after drying at the end of the 63 hours. After drying, the tops of many small features below 10 μm in size were adhered to neighboring features, presumably drawn together by capillary forces. The bottoms of these features nevertheless remained attached to the substrate.

Sample results from this test are presented in Figure 11 at a development time of 45 hours, corresponding to over-development by about 20 hours. These optical images show five-by-five arrays of square posts having lateral dimensions of 6, 8 and 10 μm for the 7, 10 and 15 μm absorber thicknesses. All of the posts remain vertical and attached to the substrate for the 10 and 15 μm absorbers. For the 7 μm absorber, 6 and 8 μm posts are detached or leaning, while the 10 μm features remain intact. This represents an average undercut rate of about 0.2 μm/h based on 20 hours of over-development. The computed interface doses for the 7 and 10 μm absorbers are 1.4 and 0.7 kJ/cm3, respectively, and these yield dissolution rates for cross-linked PMMA of about 0.2 and 0.01 μm/h. As such, loss of features in this test appears governed by the undercutting characterized in Figure 5. The minimum acceptable absorber thickness for the anodized aluminum substrate is thus at most about 10 μm for any resist thickness less than 1 mm and the exposure conditions used here. Thinner resists or a more transparent mask membrane should enable the use of a significantly smaller absorber thickness.

The images in Figure 11 are typical of this test, though anomalous loss of features did occur in a very few cases. Asterisk-like posts, for example, were successfully patterned down to 4 μm for

all absorber thicknesses, but a few of these features near the 10 μm size were lost from the substrate for the 10 μm absorber thickness. All larger and smaller posts remained for the same absorber thickness, and no such losses occurred for the thinner 7 μm absorber.

Estimated minimum absorber thicknesses for the anodized aluminum substrate are given more generally in Figure 12 as function of resist thickness for both silicon and beryllium mask membranes. Three alternative criteria determining the minimum acceptable thickness are represented in this plot. The first is the fixed undercut rate previously discussed (labeled $r_{uc} = 0.1\mu m/h$). The second is a fixed undercut distance of 1 μm for the maximum credible period of over-development [39] assuming that very small and very large features appear on the same resist ($\varepsilon_{uc} = 1$ μm). These first two criteria are both related to loss of features, while the third is tied to dimensional errors. This third criterion ($\varepsilon_{sw} = 1.1\ \varepsilon_{sw0}$) is the minimum absorber thickness yielding a top-surface sidewall offset that exceeds the smallest possible offset by only 10% [29]. The smallest possible offset is obtained when the absorber thickness is infinite.

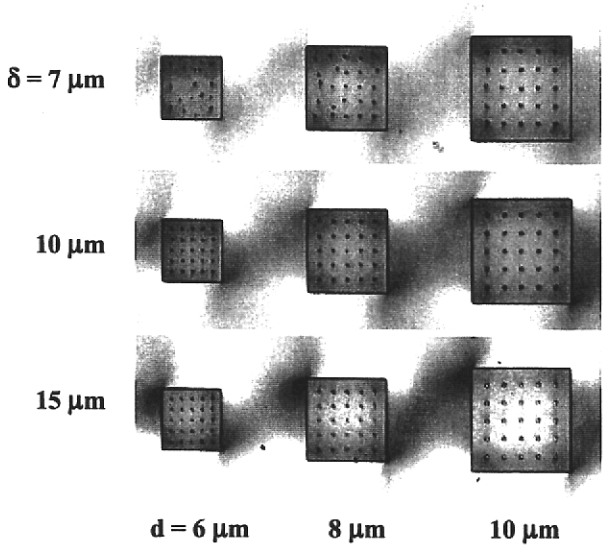

Figure 11. Optical images of post arrays patterned using a mask with absorbers of varied thickness. Posts are lost or have fallen over for only the 7 μm absorber thickness and post sizes less than 10 μm.

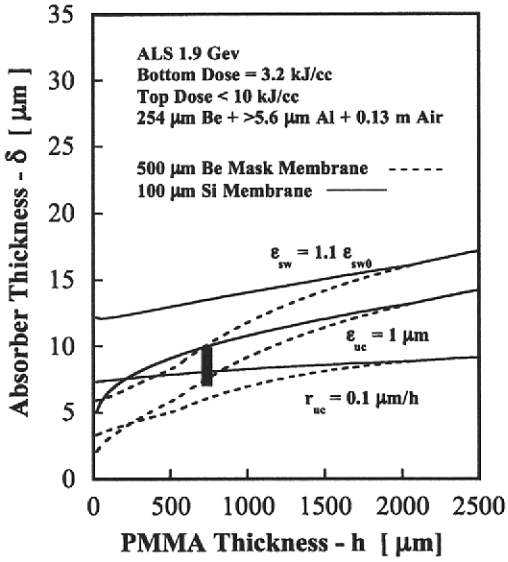

Figure 12. Computed minimum absorber thickness for the anodized aluminum substrate based on criteria of undercutting and dimensional errors. Sidewall errors provide the most stringent requirement.

The rectangular symbol in Figure 12 indicates the minimum absorber thickness of 7 to 10 μm determined from the results of Figure 11 at a resist height of 750 μm and exposure using a silicon mask membrane. This is in good agreement with the criterion based on a fixed undercut rate. However, both this criterion and that based on a fixed undercut distance give absorber thicknesses below those required for good dimensional accuracy, and this is the case for all resist thicknesses regardless of the mask membrane material. The required absorber thickness for this substrate thus ranges from about 13 to 15 μm for a silicon mask membrane and resist thicknesses of 300 to 1500 μm. It varies from 7 to 14 μm for the beryllium membrane over this range. In contrast, we presently use an absorber thickness of roughly 38 μm for the Ti-Cu-Ti substrate.

Capability in producing small resist features of high aspect ratio is further illustrated in Figure 13 depicting small features exposed and developed at a resist thickness of 2.8 mm. Exposure conditions for these results are as described for Figure 11, but the mask absorber thickness used here is uniform at 18 μm. The top panel of this figure is an optical image of the resist (still wet) following 83 hours of development. This corresponds to over-development by about 40 hours. The lower panel is an SEM image of the same features after the resist was dried. Figure 13 shows that even the 10 μm features, the smallest patterned here, survived this extensive over-development without detaching from the substrate. The aspect ratio of these smallest features is 280. Note that the tops of the smaller features have aggregated during the drying process (very top of lower panel). Despite this, the bottoms remain attached to the substrate.

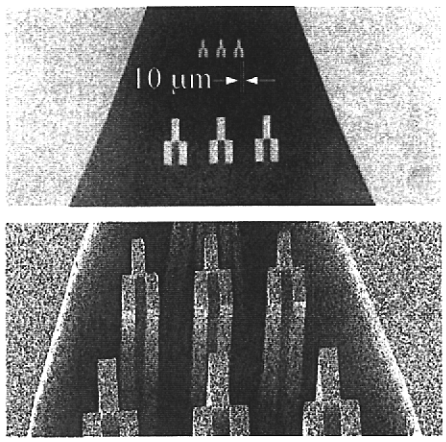

Figure 13. Optical and SEM images of resist features at a thickness of 2.8 mm and aspect ratios up to 280. The 10 μm features remained attached to the substrate despite over-development by roughly 40 hours.

Resistance to delamination is demonstrated in Figure 14. These nickel structures, formed in a thin resist, were produced using an anodized aluminum substrate bonded to the resist with PMMA glue (top panel) and a Ti-Cu-Ti substrate solvent-bonded to the resist (bottom). The resist is still present in these images. Its initial thickness was roughly 250 μm, while the height of the lapped structures is about 200 μm. Exposures for these were as described for Figure 11, except the mask membrane here was a 500 μm beryllium wafer and the absorber thickness was about 34 μm. The same mask was used for both exposures. These images show that the aluminum substrate exhibits no resist delamination, as is typical for this substrate. In contrast, the Ti-Cu-Ti substrate shows extensive delamination near the perimeter of the resist and on the interior. This is likewise typical of the Ti-Cu-Ti substrate for thin resists exposed at ALS, though delamination for Ti-Cu-Ti is sometimes much less pronounced.

Figure 15 illustrates success in producing metal structures using the anodized aluminum substrate. These are all nickel parts that have been planarized by lapping. The height of the structure in panel A is 190 μm, and the minimum width of the main vertical flexure is 51 μm. This structure was fabricated using a transparent mask membrane and an absorber thickness of just 8 to 10 μm. Panel B shows fine negative features down to 10 μm at a finished height of 700 μm and an aspect ratio of 70. This is the largest aspect ratio attempted to date in a metal part. Negative circular features at a diameter of roughly 15 μm were produced at the same time. Lapped nickel structures at a height of 300 μm are shown in panel C. The flexure near the

bottom has a width of 30 μm; the diameter of the two small registration holes is 50 μm. Finally, panel D depicts a thick structure at a height of 1400 μm. The width of the curved flexure is about 140 μm. Each of the structures shown in Figure 15 was successfully produced on the first attempt.

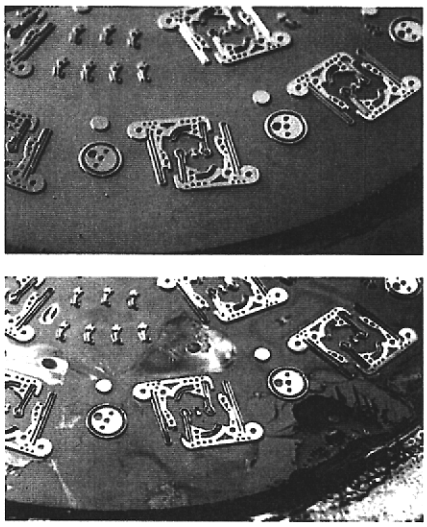

Figure 14. Optical images of nickel structures and PMMA resist on a wafer. Top image (anodized aluminum) shows no delamination; bottom image (Ti-Cu-Ti) shows widespread detachment of resist.

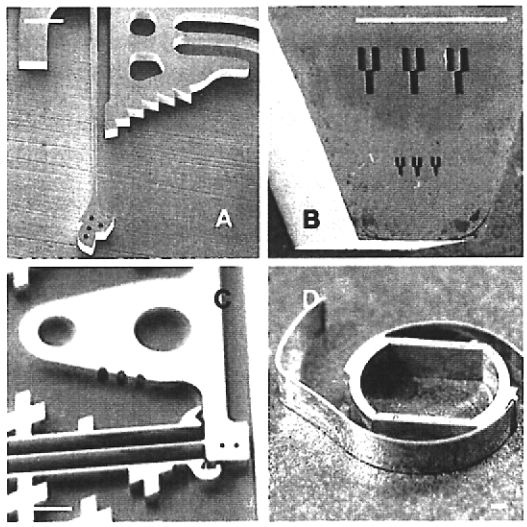

Figure 15. Nickel structures produced using the anodized aluminum substrate. Images illustrate isolated negative features down to 10 μm and structure heights to 1400 μm. Scale bar lengths are all 500 μm.

Summary

The analyses presented here show that the minimum absorber thickness required to avoid loss of features and resist delamination varies by up to a factor of five depending on the substrate material and the acceptable shadow-region resist dose at the substrate interface. Based on these analyses, we propose and demonstrate that the maximum interface dose for which feature loss does not occur may be determined by degradation of bond strength, a stringent requirement, or by allowable undercut rates if the initial bond strength is high. For conditions typical of LIGA, the minimum absorber thickness yielding an acceptable undercut rate ranges from 4 μm for carbon and beryllium substrates to about 22 μm for copper. It is just less than 10 μm for aluminum oxide. We also demonstrate that the minimum absorber thickness based on the undercut rate is sufficiently small for aluminum and carbon substrates that the required absorber thickness is instead determined by primary dose contrast and sidewall dimensional errors.

These analyses additionally indicate that bright-region resist doses at the substrate interface can approach 100 kJ/cm^3 for copper, nickel and zinc substrates, likely requiring a post-development etch to remove insoluble resist adjacent to the substrate. Bright-region interface doses for titanium oxide, aluminum and aluminum oxide are sufficiently low that etching is not required. Finally, we show that maximum resist shadow-region doses due to fluorescence from the substrate are sufficiently large to produce significant sidewall errors for copper, zinc, nickel and

titanium substrates, at least under some conditions. Those for titanium oxide, aluminum and aluminum oxide are too low to produce such errors.

In keeping with these expectations, our adhesion experiments confirm that loss of features during development is reduced significantly using substrate materials having low x-ray cross-sections. Studies using solvent-bonded resists indicate that carbon substrates exhibit minimal feature loss, aluminum and titanium show small to moderate loss, and substrates metallized with Ti-Cu-Ti yield dramatic feature loss beginning immediately upon full development. These studies also revealed that the solvent-bonding process frequently produces anomalous loss of large features before smaller features detach. This behavior was very rare for resists bonded using PMMA-based glue. Pull-tests of bonded PMMA tabs, conducted without x-ray exposure, establish that surface preparation and especially surface roughness are critical to obtaining high initial bond strength.

The present studies of electrodeposition focused on carbon and aluminum substrates. We found that vitreous carbon disks and carbon-coated wafers give generally poor nucleation and poor adhesion of deposited metals. Several approaches were investigated for electrodeposition on aluminum, including a post-development through-mold zincate treatment, post-development anodization, and anodization prior to bonding the resist. The deposition of extremely thin zinc layers prior to resist bonding was also examined. Of these approaches, anodization prior to bonding proved to be most successful, and a trace concentration of copper and silicon in the aluminum (>1% weight) was identified as key to this success. Anodizing either aluminum films or discs of the proper alloy composition at 32 °C using phosphoric acid and an applied potential of 75 V provide good nucleation and good adhesion of the deposited metal. Anodizing the aluminum before bonding the resist provides the additional benefit of fine-scale surface roughness for good adhesion of the resist.

The practical result of these studies is a new anodized aluminum substrate for use in LIGA. This substrate provides high initial bond strength for the PMMA resist, low resist interface doses, low fluorescence doses, and a surface enabling good nucleation and adhesion of the electrodeposited metal. No bright-region layer of insoluble resist is produced on the substrate surface so a post-development etch is not required, and this opens the possibility of transferring the developed resist into an electrolyte bath without drying. Based on calculations and one preliminary test, the minimum absorber thickness for this substrate appears to be less than 15 μm for most conditions typical of LIGA. The required absorber thickness may be as small as 7 μm for thin resists exposed using a transparent mask membrane.

Loss of fine features and resist delamination are essentially eliminated using the new substrate when the resist is bonded using PMMA-based glue, even for over-development by several days and long periods of electrodeposition. This has been demonstrated through successful exposure and development of 6 μm features a height of 750 μm and 10 μm features at a height of 2.8 mm. Success in electrodeposition was demonstrated through fabrication of lapped nickel structures containing small negative features at heights of 190 to 1400 μm.

Acknowledgment

The authors thank G. D. Kubiak for his support and encouragement of this work. We also thank A. D. Gardea, J. M. Chames J. L. Yio and K. L. Krafcik for their invaluable contributions of optical and SEM microscopy. This work was funded in part by Sandia's Materials Science Research Foundation and in part by the Sandia LIGA Technical Maturation Project. Sandia is a multiprogram laboratory operated by Sandia Corporation, a Lockheed Martin Company, for the United States Department of Energy under contract DE-AC04-94AL85000. The Advanced Light Source is supported by the Director, Office of Science, Office of Basic Energy Sciences, Materials Sciences Division, of the U.S. Department of Energy under Contract No. DE-AC03-76SF00098 at Lawrence Berkeley National Laboratory.

References

1. E. W. Becker, W. Ehrfeld, P. Hagmann, A. Maner, D. Munchmeyer, "Fabrication of Microstructures with High Aspect Ratios and Great Structural Heights by Synchrotron Radiation Lithography, Galvanoforming and Plastic Moulding (LIGA Process)," *Microelectronic Eng.*, **4**, 35-56, 1986.

2. D. Munchmeyer and W. Ehrfeld, "Accuracy Limits and Potential Applications of the LIGA Technique in Integrated Optics," Proceedings of the SPIE, *Micromachining of Elements with Optical and other Submicrometer Dimensional and Surface Specification,* **803**, 72-79, 1987.

3. W. Ehrfeld, P. Bley, F. Gotz, J. Mohr, D. Munchmeyer, W. Schelb, H. J. Baving, D. Beets, "Progress in Deep-Etch Synchrotron Radiation Lithography," *J. Vac. Sci. Technol. B*, **6**, 178-182, 1988.

4. F. J. Pantenburg, J Chlebeck, A. El-Kholi, H. L. Huber, J. Mohr, H. K. Oertel, J. Schultz, "Adhesion Problems in Deep-Etch X-ray Lithography Caused by Fluorescence Radiation from the Plating Base," *J. Microelectronic Eng.*, **23**, 223-226, 1994.

5. A. Schmidt, A. Clifton, W. Ehrfeld, G. Feiertag, H. Lehr and M. Schmidt, "Investigation of the Adhesive Strength of PMMA Structures on Substrates Obtained by Deep X-Ray Lithography," *J. Microelectronic. Eng.*, **30**, 215-218, 1996.

6. H. Zumaque, G. A. Kohring and J. Hormes, "Simulation Studies of Energy Deposition and Secondary Processes in Deep X-Ray Lithography," *J. Micromech. Microeng.*, **7**, 79-88, 1997.

7. F. J. Pantenburg and J. Mohr, "Influence of Secondary Effects on the Structure Quality in Deep X-Ray Lithographie," *Nucl. Instrum. Methods Phys. Res. B*, **97**, 551-556, 1995.

8. F. J. Pantenburg, S. Achenbach and J. Mohr, "Characterization of Defects in Very High Deep-Etch X-Ray Lithography Microstructures," *Microsyst. Technol.*, **4**, 89-93, 1998.

9. G. Feiertag, W. Ehrfeld, H. Lehr, A. Schmidt and M. Schmidt, "Calculation and Experimental Determination of the Structure Transfer Accuracy in Deep X-Ray Lithography," *J. Micromech. Microeng.*, **7**, 323-331, 1998.

10. S. K. Griffiths and A. Ting, "The Influence of X-Ray Fluorescence on LIGA Sidewall Tolerances," *Microsyst. Technol.*, **8**, 120-128, 2002.

11. J. Mohr, Ehrfeld and D. Munchmeyer, "Requiremets on Resist Layers in Deep-Etch Synchrotron Radiation Lithography," *J. Vac. Sci. Technol. B*, **6**, 2264-2267, 1988.

12. H. Guckel, K. J. Skrobis, T. R. Christenson, J. Klein, S. Han, B. Choi, E. G. Lovell and T. W. Chapman, "Fabrication and Testing of the Planar Magnetic Motor," *J. Micromech. Microeng.*, **1**, 135-138, 1991.

13. H. Guckel, "Formation of Microstructures by Multiple Level Deep X-Ray Lithography with Sacrificial Metal Layers," U.S. Patent Number 5,190,637, 1993.

14. H. Guckel, T. R. Christenson and K. J. Skrobis, "Formation of Microstructures using a Preformed Photoresist Sheet," U.S. Patent Number 5,378,583, 1995.

15. H. Guckel, T. R. Christenson and K. J. Skrobis, "Formation of Microstructures using a Preformed Photoresist Sheet," U.S. Patent Number 5,496,668, 1996.

16. H. Guckel, T. R. Christenson and K. J. Skrobis, "Formation of Microstructures using a Preformed Photoresist Sheet," U.S. Patent Number 5,576,147, 1996.

17. H. Guckel, J. L. Klein and T. L. Earles "Micromechanical Magnetically actuated Devices," U.S. Patent Number 5,644,177, 1997.

18. D. Kadereit, J. Hormes, G. Mohn and A. El-Kohli, "Studies of the Adhesion Properties of LIGA Microstructures by X-Ray Spectroscopy and Mechanical Measurement," *Microsyst. Technol.*, **2**, 71-74, 1996.

19. C. G. Khan Malek and S. S. Das, "Adhesion Promotion Between Poly(Methylmethacrylate) and Metallic Surfaces for LIGA Evaluated by Shear Stress Measurements," *J. Vac. Sci. Technol B.*, **16**, 3543-3546, 1998.

20. V. K. P. Kanigicheri, K. W. Wally, E. Ma, W. Wang and M. C. Murphy, "Enhanced Adhesion of PMMA to copper with Black Oxide for Electrodposition of High Aspect Ratio Nickel-Iron Microstructures," *Microsyst. Technol.*, **4**, 77-81, 1998.

21. F. De Carlo, J. J. Song and D. C. Mancini, "Enhanced Adhesion Buffer Layer for Deep X-Ray Lithography," *J. Vac. Sci. Technol. B*, **16**, 3539-3542, 1998.

22. S. S. Bajikar, F. De Carlo, J. J. Song "Enhanced Adhesion for LIGA Microfabrication by using a Buffer Layer," U.S. Patent Number 6,277,539, 2001.

23. S. S. Bajikar, F. De Carlo, J. J. Song "Enhanced Adhesion for LIGA Microfabrication by using a Buffer Layer," U.S. Patent Number 6,682,870, 2004.

24. T. Kunz, J. Mohr, A. Ruzzu, K. D. Skrobanek and U. Wallrabe, "Adhesion of Ni Structures on AL2O3 Ceramic Substrates used for the Sacrificial Layer Technique," *Microsyst. Technol.*, **6**, 121-125, 2000.

25. A. El-Kholi, K. Bade, J. Mohr, F. J. Pantenburg and X. M. Tang, "Alternate Resist Adhesion and Electroplating Layers for LIGA Process," *Microsyst. Technol.*, **6**, 161-164, 2000.

26. O. V. Makarova, D. C. Mancini, N. Moldovan, R. Divan, C. M. Tang, D. G. Ryding and R. H. Lee, "Microfabrication of Freestanding Metal Structures using Graphite Substrate," *Sens. Actuators A*, **103**, 182-186, 2003.

27. F. Perennes and F. J. Pantenburg, "Adhesion Improvement in the Deep X-Ray Lithography Process using a Central Beam Stop," *Nucl. Instrum. Methods Phys. Res. B*, **174**, 317-323, 2001.

28. S. K. Griffiths, J. M. Hruby and A. Ting, "The influence of Feature Sidewall Tolerance on Minimum Absorber Thickness for LIGA X-Ray Masks," *J. Micromech. Microeng.*, **9**, 353-361, 1999.

29. S. K. Griffiths, "Fundamental Limitations of LIGA X-Ray Lithography: Sidewall Offset, Slope and Minimum Feature Size," *J. Micromech. Microeng.*, **14**, 999-1011, 2004.

30. F. J. Pantenburg, S. Achenbach and J. Mohr, "Influence of Developer Temperature and Resist Material on the Structure Quality in Deep X-Ray Lithography," *J. Vac. Sci. Technol B.*, **16**, 3547-3551, 1998.

31. E. M. Lehockey, J. D. Wice and I. Reid, "Dissolution Characteristics of Poly(Methyl Methacrylate) as an X-Ray Resist," *Can. J. Phys.*, **65**, 975-979, 1987.

32. B. Chaudhuri, H. Guckel, J. Klein and K. Fischer, "Photoresist Application for the LIGA Process," *Microsyst. Technol.*, **4**, 159-162, 1998.

33. F. J. Pantenburg, Research Center Karlsruhe (FZK), private communication.

34. S. K. Griffiths, J. A. W. Crowell, B. L. Kistler and A. S. Dryden, "Dimensional Errors in LIGA-Produced Metal Structures due to Thermal Expansion and Swelling of PMMA," *J. Micromech. Microeng.*, **14**, 1548-1557, 2004.

35. A. Ruzzu and B. Matthis, "Swelling of PMMA Structures in Aqueous Solutions and Room Temperature Ni-Electroforming," *Microsyst. Technol.*, **8**, 116-119, 2002.

36. S. H. Goods, R. M. Watson and M. Yi, "Thermal Expansion and Hydration Behavior of PMMA Molding Materials for LIGA Applications," Sandia National Laboratories Report SAND2003-8000, 2003.

37. K. R. Van Horn, ed., *Aluminum - Vol III Fabrication and Finishing*, chapter 20, American Society for Metals, Metals Park, OH, 1967.

38. D. S. Lashmore, "AES Research Project-41: Plating on Anodized Aluminum," *Plating and Surface Finishing*, **68**, 48-51, 1981.

39. S. K. Griffiths and R. H. Nilson, "Transport Limitations on Development Times of LIGA PMMA Resists," *Microsyst. Technol.*, **8**, 335-342, 2002.

Distribution

B. L. Dearth MS-FH40
Honeywell Federal Manufacturing
& Technologies
PO Box 419159
Kansas City, MO 64141

T. Casey MS-1C41
Honeywell Federal Manufacturing
& Technologies
PO Box 419159
Kansas City, MO 64141

R. Steinhoff MS-1C41
Honeywell Federal Manufacturing
& Technologies
PO Box 419159
Kansas City, MO 64141

M. Widmar MS-MD40
Honeywell Federal Manufacturing
& Technologies
PO Box 419159
Kansas City, MO 64141

L. Zawiki MS-MD40
Honeywell Federal Manufacturing
& Technologies
PO Box 419159
Kansas City, MO 64141

V. Saile
Institut fur Mikrostrukturtechnik
Forschungszentrum Karlsruhe
Hermann-von-Helmholtz-Platz 1
76344 Eggenstein-Leopoldshafen
Germany

J. Mohr
Institut fur Mikrostrukturtechnik
Forschungszentrum Karlsruhe
Hermann-von-Helmholtz-Platz 1
76344 Eggenstein-Leopoldshafen
Germany

F. J. Pantenburg
Institut fur Mikrostrukturtechnik
Forschungszentrum Karlsruhe
Hermann-von-Helmholtz-Platz 1
76344 Eggenstein-Leopoldshafen
Germany

S. Achenbach
TRLabs
111-116 Research Drive
Saskatoon, SK S7N3R3
Canada

P. Meyer
Institut fur Mikrostrukturtechnik
Postfach 3640
76021 Karlsruhe
Germany

R. A. Lawes
Imperial College, London
Dept. of Electrical and Electronic Engr.
Exhibition Road, South Kensington Campus
London SW72AZ
United Kingdom

1415 J. C. Barbour, 1112
1415 T. A. Friedmann, 1112
1077 T. E. Zipperian, 1740
0603 J. J. Hudgens, 1743
0603 T. Lemp, 1743
0603 W. C. Sweatt, 1743
1425 W. G. Yelton, 1743
0877 M. J. Cieslak, 1800
Attn: R. J. Salzbrenner, 1801
G. S. Heffelfinger, 1802
0340 A. Hall, 1832
1411 V. Tikare, 1834
0889 J. S. Custer, 1851
0889 T. E. Buchheit, 1851
0889 M. T. Dugger, 1851
0889 S. V. Prasad, 1851
0865 D. L. Cook, 1900

0865 C. C. Henderson, 1902
0503 D. W. Plummer, 2330
0319 J. R. Fellerhoff, 2610
0311 M. J. Craig, 2613
0319 R. E. Kreutzfeld, 2613
0319 G. T. Randall, 2613
1310 E. J. Garcia, 2614
1310 M. A. Polosky, 2614
1310 G. E. Sleefe, 2614
0311 L. L. Lukens, 2618
0311 D. E. Petersen, 2618
0311 C. W. Vanecek, 2618
0311 R. Wild, 2618
0437 J. M. McGlaun, 2830
9001 M. E. John, 8000
Attn: R. H. Stulen, 8100
K. E. Washington, 8900
9054 T. A. Michalske, 8300
Attn: L. M. Napolitano, 8320
D. R. Hardesty, 8360
9054 R. W. Carling, 8350
9007 D. R. Henson, 8200
Attn: G. A. Thomas, 8220
B. K. Damkroger, 8240
9401 G. F. Cardinale, 8245
9042 S. K. Griffiths, 8350
9403 J. M. Hruby, 8700
9401 G. D. Kubiak, 8750
9055 S. W. Allendorf, 8753
9401 M. A. Hekmaty, 8753
9401 L. L. Hunter, 8753
9401 G. Aigeldinger, 8753
9401 D. R. Boehme, 8753
9401 J. T. Ceremuga, 8753
9401 J. T. Hachman, 8753
9401 J. J. Kelly, 8753
9401 M. W. Losey, 8753
9401 D. E. McLean, 8753
9401 M. E. Malinowski, 8753
9401 S. Mrowka, 8753
9401 P. C. Y. Yang, 8753
9401 D. M. Skala, 8753
9409 S. H. Goods, 8754
9409 J. S. Korellis, 8754
9409 P. A. Spence, 8754
9161 W. R. Even, 8760
9161 D. L. Medlin, 8761
9403 L. A. Domeier, 8762
9401 A. M. Morales, 8762
9161 E. P. Chen, 8763
9042 R. H. Nilson, 8764
9401 A. A. Talin, 8764
9401 T. I. Wallow, 8764
9402 K. L. Wilson, 8770
Attn: J. C. F. Wang, 8773
9402 J. E. M. Goldsmith, 8772
9403 B. E. Mills, 8773
9403 N. Y. C. Yang, 8773
9042 G. H. Evans, 8775
9042 R. S. Larson, 8775
9042 C. D. Moen, 8775
9042 A. Ting, 8775
0825 W. L. Hermina, 9110
1310 S. N. Kempka, 9113
0834 J. S. Lash, 9114
0834 H. K. Moffat, 9114

9018 Central Technical Files, 8940-2
0899 Technical Library, 4916
9021 Technical Communications, 8528
9021 Technical Communications, 8815
for DOE/OSTI